

## Accepted Manuscript

High activity magnetic core-mesoporous shell sulfonic acid silica nanoparticles for carboxylic acid esterification

Zhijun Tai, Mark A. Isaacs, Christopher M.A. Parlett, Adam F. Lee, Karen Wilson

PII: S1566-7367(17)30013-4  
DOI: doi: [10.1016/j.catcom.2017.01.004](https://doi.org/10.1016/j.catcom.2017.01.004)  
Reference: CATCOM 4903

To appear in: *Catalysis Communications*

Received date: 8 November 2016  
Revised date: 28 December 2016  
Accepted date: 4 January 2017

Please cite this article as: Zhijun Tai, Mark A. Isaacs, Christopher M.A. Parlett, Adam F. Lee, Karen Wilson, High activity magnetic core-mesoporous shell sulfonic acid silica nanoparticles for carboxylic acid esterification. The address for the corresponding author was captured as affiliation for all authors. Please check if appropriate. *Catcom*(2017), doi: [10.1016/j.catcom.2017.01.004](https://doi.org/10.1016/j.catcom.2017.01.004)

This is a PDF file of an unedited manuscript that has been accepted for publication. As a service to our customers we are providing this early version of the manuscript. The manuscript will undergo copyediting, typesetting, and review of the resulting proof before it is published in its final form. Please note that during the production process errors may be discovered which could affect the content, and all legal disclaimers that apply to the journal pertain.

## High activity magnetic core-mesoporous shell sulfonic acid silica nanoparticles for carboxylic acid esterification

*Zhijun Tai, Mark A. Isaacs, Christopher M.A. Parlett, Adam F. Lee and Karen Wilson,\**

European Bioenergy Research Institute, Aston University, Birmingham, B4 7ET, UK.

\*Corresponding Author: Tel.: +44 (0) 121 204 5456; Email address: k. wilson@aston.ac.uk

### ABSTRACT:

Magnetically-separable solid acid nanoparticle catalysts, comprising 80 nm Fe<sub>3</sub>O<sub>4</sub> cores, a thin, dense silica inner shell and a mesoporous sulfonic acid silica outer shell, have been synthesized through a surfactant-templating and hydrothermal saline-promoted grafting protocol. These porous nanocomposites offer excellent activity towards propanoic acid esterification, in combination with facile recovery and re-use.

KEYWORDS: magnetic nanoparticles, core-shell, mesoporous, sulfonic silica, esterification

### 1. INTRODUCTION

Catalytic transformations require the combination of highly active materials with ease of separation and product recovery. Heterogeneous catalysts can offer a facile solution to separation via facile filtration/settling of micron-scale materials, but unfortunately suffer from poor reaction rates relative to homogeneous counterparts due to diffusion limitations. Diffusion-limited mass

transport is particularly problematic for liquid phase transformations of bulky or viscous reactants employing conventional microporous catalysts.[1] While nanoparticle catalysts offer enhanced activity, their practical application is restricted due to requirements for energy-intensive separation through centrifugation. The challenge of designing high activity catalytic nanoparticles which can be easily recovered is driving the search for magnetically-separable catalysts for use in a range of applications spanning photocatalysis, biomass conversion, environmental pollution control and synthetic organic chemistry.[2]

The application of core-shell, magnetically separable silica microspheres has attracted significant interest in recent years due to their magnetic response and versatile derivatization of the silica shell. [3] Such dispersible, nanoscale magnetic solid acid catalysts are particularly attractive for improving product separation/catalyst recovery and associated process engineering of liquid phase biomass transformations including cellulose hydrolysis,[4] fructose dehydration,[5] aldol condensation of 5-hydroxymethylfurfural (5-HMF) with ethanol,[6] oxidation of 5-HMF to 2,5-diformylfuran,[7] and biodiesel production. [8, 9]

The development of high activity and readily separable solid acid catalysts for carboxylic acid esterification would be highly desirable in the context of bio-oil upgrading to sustainable fuels. Bio-oils generated from thermal processing of waste agricultural or forestry biomass are highly corrosive due to the presence of high levels of short chain acids [10] which prohibit its direct use as a fuel. Pre-treatment of the raw pyrolysis bio-oil [11] via solid acid catalyzed esterification to neutralize acetic and propanoic acid components is an energy efficient and atom-economical means to improve bio-oil quality. [12] Catalyst separation from, and molecular diffusion within,

viscous bio-oils remains a challenge for this upgrading approach, necessitating porous solid acids with high acid site loadings and a simple property to aid their extraction from the bio-oil.

Conventional routes to prepare magnetically separable catalysts generate materials with non-porous shells, which typically comprise either large (>500 nm), low surface area nanoparticles,[13, 14] or nanoparticle aggregates rather than discrete nanostructures which hinders their derivatization resulting in low active site loadings and associated catalytic efficiency. [15, 16] Analogues possessing mesoporous silica shells have been developed recently as MRI contrast agents [17, 18] and for drug delivery. [19] Here we adapt such methodologies to fabricate the first monodispersed, magnetic core-mesoporous shell solid acid nanocatalysts. These possess high surface areas (>300 m<sup>2</sup>·g<sup>-1</sup>), superior mass transport to conventional mesoporous SBA-15 silica counterparts (which suffer from micron-length pore channels), and high sulfonic acid loadings, which in concert afford efficient propanoic acid esterification and subsequent facile magnetic separation.

## 2. EXPERIMENTAL

### Catalyst preparation

Silica encapsulated magnetic iron oxide nanoparticles were synthesized by adapting the method of Zhao et al.[19] Uniform hematite (Fe<sub>2</sub>O<sub>3</sub>) particles were obtained by ageing FeCl<sub>3</sub> aqueous solution (0.02 M) at 100 °C for 48 h. The resulting Fe<sub>2</sub>O<sub>3</sub> nanoparticles were washed and separated via centrifugation with 2-propanol three consecutive times. Subsequently, 500 mg of Fe<sub>2</sub>O<sub>3</sub> nanoparticles was added to a mixture of 2-propanol (800 mL), H<sub>2</sub>O (160 mL) and concentrated aqueous NH<sub>3</sub> (35 %, 20 mL), to which tetraethyl orthosilicate (TEOS, 0.74g) was then added dropwise under vigorous stirring prior to ageing at room temperature for 15 h. The

resulting  $\text{Fe}_2\text{O}_3@\text{SiO}_2$  nanoparticles were centrifuged and dried, and 50 mg of these re-dispersed in a solution of ethanol (12 mL),  $\text{H}_2\text{O}$  (2 mL) and aqueous  $\text{NH}_3$  (35 %, 0.8 mL). To this mixture, 0.3 mL of TEOS and C18TMS were added quickly (in a molar ratio of 4.7:1) under vigorous stirring at room temperature, prior to ageing overnight. The resulting nanoparticles were collected by centrifugation, and calcined subsequently at 550 °C for 6 h to remove the organic template (C18TMS) and form a mesoporous silica shell. Finally, magnetic  $\text{Fe}_3\text{O}_4@\text{SiO}_2@m\text{SiO}_2$  core-shell nanoparticles were obtained by 450 °C reduction in  $\text{H}_2$  for 4 h.

Sulfonic acid functionalized  $\text{Fe}_3\text{O}_4@\text{SiO}_2@m\text{SiO}_2$  nanoparticles were prepared via two post-grafting methods, employing either toluene or saline as the solvent. For the former, 0.5 g of the  $\text{Fe}_3\text{O}_4@\text{SiO}_2@m\text{SiO}_2$  nanoparticles were added into 30 mL of toluene (Fisher 99 %) containing 0.5 mL of mercaptopropyl trimethoxysilane (MPTMS, 95 % Alfa Aesar) followed by reflux at 130 °C under stirring for 24 h. The resulting thiol-functionalized nanoparticles were magnetically separated, washed three times with 100 mL methanol (Fisher 99 %) and dried at 80 °C. Thiol groups were converted into  $-\text{SO}_3\text{H}$  functions by mild oxidation with 25 mL of hydrogen peroxide (30 %, Sigma-Aldrich) under continuous stirring at room temperature for 24 h. The resulting propylsulfonic acid functionalized  $\text{Fe}_3\text{O}_4@\text{SiO}_2@m\text{SiO}_2$  were subsequently separated by a magnet, washed three times with methanol and dried at 80 °C. These are indicated by a (toluene) suffix. Alternatively, the functionalization of MPTMS was performed through hydrothermal saline promoted grafting (HSPG), in which 0.5g of  $\text{Fe}_3\text{O}_4@\text{SiO}_2@m\text{SiO}_2$  nanoparticles were added to 30 mL  $\text{H}_2\text{O}$  solvent containing of 0.1 g of NaCl and 0.5 mL of MPTMS and refluxed at 100 °C under stirring for 24 h. Thiol oxidation was performed as for the conventional toluene method above. These are indicated by a (HSPG) suffix. Non-mesoporous magnetic solid acid catalysts were prepared employing the same (HSPG and conventional

toluene) functionalization methods, but using  $\text{Fe}_3\text{O}_4@\text{SiO}_2$  nanoparticles prepared as above (i.e. without the additional second mesoporous silica layer).

SBA-15 was synthesized adopting the protocol of Zhao and co-workers. [20] 10 g of Pluronic P123 triblock copolymer was dissolved in 75 ml of water and 250 ml of 2 M HCl solution. The mixtures were stirred at 35 °C for dissolution and then 23 ml of TEOS were added, maintained at 35 °C for 20 h under stirring. The resulting gel was then aged at 80 °C for 24 h. Finally, the solid product was filtered, washed with water and calcined statically in air at 550 °C for 5 h. Sulfonation was performed in toluene as described above.

### **Catalyst characterization**

Structural properties were determined through  $\text{N}_2$  porosimetry and transmission electron microscopy (TEM). Nitrogen physisorption was undertaken on a Quantachrome Nova 1200 instrument, with samples degassed at 120 °C for 6 h prior to recording adsorption/desorption isotherms. Brunauer–Emmett–Teller (BET) surface areas were calculated over the relative pressure range 0.01–0.2 ( $p/p_0$ ), while pore size distributions were calculated using the Barrett–Joyner–Halenda (BJH) method applied to the desorption branch of the isotherm. Scanning transmission electron microscopy (STEM) and high angle annular dark field scanning transmission electron microscopy (HAADF) images were recorded on an aberration corrected JEOL 2100-F electronic microscope operating at 200 kV; equipped with a Gatan Orius SC600A CCD camera. Samples were prepared by dispersion in ethanol and drop-casting onto a copper grid coated with a holey carbon support film (Agar Scientific Ltd). Images were analysed using ImageJ 1.41 software.

Bulk and surface sulfur loadings were determined by elemental analysis and X-ray photoelectron spectroscopy respectively. The bulk sulfur elemental analysis was performed on a FLASH 2000 CHNS/O organic elemental analyzer. XPS was performed on a Kratos Axis HSi X-ray photoelectron spectrometer fitted with a charge neutralizer and magnetic focusing lens employing Al K $\alpha$  monochromated radiation (1486.7 eV); spectral fitting was performed using Casa XPS version 2.3.15, with energy referencing to the C 1s peak of adventitious carbon at 284.6eV. S 2p XP spectra was fitted using a common Gaussian/Lorentzian peak shape.

Acid site loadings were determined by thermogravimetric analysis coupled with mass spectrometry (TGA-MS). Samples were first impregnated to wetness with propylamine, and then dried in vacuo at 40 °C overnight. TGA was performed on a Mettler Toledo, TGA/DSC2 Star system with a heating rate of 10 °C·min<sup>-1</sup> from 40-800 °C under N<sub>2</sub> flow (30 mL·min<sup>-1</sup>). Evolved gas analysis was performed with a ThermoStar mass spectrometer connected to the TGA outlet by capillary heated to 180 °C. Ion currents were recorded for the strongest mass fragments of NH<sub>3</sub> (m/z 17), unreacted propylamine (m/z 30 and 59), and reactively-formed propene (m/z 41) and SO<sub>2</sub> (m/z 64) formed over acid sites.

Brönsted/Lewis acid character was determined via Diffuse Reflectance Infrared Fourier Transform Spectroscopy (DRIFTS) on a Thermo Scientific Nicolet iS50 FT-IR Spectrometer with MCT detector and Smart Collector accessory. Catalysts were diluted with KBr powder (10 wt%) and then dried in vacuo at 120 °C for 6 h. Samples were then impregnated to wetness with

pyridine, and excess pyridine removed overnight in vacuo at 30 °C prior to subsequent in vacuo DRIFTS analysis at 50 °C.

### Catalytic esterification

Esterification was carried out on a Radleys Starfish carousel at 60 °C under atmospheric pressure in a three-neck round-bottomed glass flask. Reactions employed 10 mmol propanoic acid in 12.5 mL of methanol (molar ratio  $n_{\text{MeOH}}/n_{\text{PA}} = 30$ ), 100 mg of catalyst and 0.59 mL of dihexylether as an internal standard. Samples were withdrawn periodically, separated with a strong magnet, and diluted with methanol prior to analysis on a gas chromatograph (Varian 450-GC, Phenomenex ZB-50 15 m  $\times$  0.53 mm  $\times$  1.0  $\mu\text{m}$  capillary column, TCD detector).

## 3. RESULTS AND DISCUSSION

Magnetic hematite nanoparticles encapsulated by a thin, dense silica layer were first prepared following the method of Zhao et al [19] (**Figure 1**) used previously to prepare drug delivery materials. The dense silica ( $\text{SiO}_2$ ) layer serves to protect the underlying iron oxide core from leaching in acidic environments and oxidation during the final synthetic step (in which grafted thiols are converted to sulfonic acid groups) which would result in the loss of magnetic response. Successful genesis of these  $\text{Fe}_2\text{O}_3@\text{SiO}_2$  nanoparticles was evidenced by TEM (**Figure 1a-b**), wherein uniform approximately 80 nm diameter iron oxide cores and thin ( $\sim 15$  nm), dense silica overlayers possessing limited microporosity (**Figure S2a-b**), can be readily distinguished. Formation of a final mesoporous silica shell was achieved through treatment of  $\text{Fe}_2\text{O}_3@\text{SiO}_2$  nanoparticles with TEOS and n-octadecyl-trimethoxysilane (C18TMS) and calcined at 550°C to

impart mesoporosity. Materials were finally reduced to fully convert the core to magnetic  $\text{Fe}_3\text{O}_4$  and form  $\text{Fe}_3\text{O}_4@\text{SiO}_2@m\text{SiO}_2$  nanoparticles as confirmed by powder XRD (**Figure S1**). Bright- and dark-field **Figure 1c** shows that the resulting materials are monodispersed with a sandwich core-shell structure comprising a dense inner and less dense  $\sim 60$  nm outer silica shell. Porosimetry confirmed that the outer shell imparted mesoporosity to the nanoparticles, associated with the presence of uniform 3 nm diameter mesopore channels (**Table 1, Figure S2c-d**) and an increase in BET surface area from  $45 \text{ m}^2\cdot\text{g}^{-1}$  to  $420 \text{ m}^2\cdot\text{g}^{-1}$ .

Sulfonic acid functionalization of both the  $\text{Fe}_2\text{O}_3@\text{SiO}_2$  and  $\text{Fe}_3\text{O}_4@\text{SiO}_2@m\text{SiO}_2$  nanoparticles was subsequently attempted via grafting of (3-mercaptopropyl)trimethoxysilane (MPTS) using either a conventional (toluene) or hydrothermal saline promoted grafting (HSPG) approach [21] prior to thiol oxidation by  $\text{H}_2\text{O}_2$ . The HSPG method was recently shown to significantly enhance propyl sulfonic acid loadings over SBA-15 [21] and periodic mesoporous organo-silicas; [22] this work represents its first application to functionalizing core-shell structures. TEM imaging of the  $\text{Fe}_3\text{O}_4@\text{SiO}_2@m\text{SiO}_2$  (HSPG) material confirmed retention of the sandwich structure and mesoporous shell following HSPG grafting and energy dispersive X-ray spectroscopy (EDX) confirmed the presence of sulfur (**Figure 1d-e**). A decrease in the pore volume and average BJH pore diameter was observed following grafting of the mesoporous shell nanoparticles (**Table 1**), indicative of MPTS incorporation throughout the entire pore network, however the  $\text{Fe}_3\text{O}_4@\text{SiO}_2@m\text{SiO}_2$  materials retained high surface areas exceeding  $300 \text{ m}^2\cdot\text{g}^{-1}$ . Bulk and surface elemental analysis, and acid site titration confirmed that the mesoporous  $\text{Fe}_3\text{O}_4@\text{SiO}_2@m\text{SiO}_2$  exhibited significantly higher sulfur content than  $\text{Fe}_2\text{O}_3@\text{SiO}_2$ , with the HSPG sulfonic acid route conferring superior sulfur and acid site loadings. A maximum S

content of 1.35 wt% and acid site loading of  $0.51 \text{ mmol}\cdot\text{g}^{-1}$  was obtained for  $\text{Fe}_3\text{O}_4@\text{SiO}_2@m\text{SiO}_2$  (HSPG). S 2p XP spectra confirmed that sulfur was fully oxidised in all functionalized materials, with a single chemical environment at 169.2 eV binding energy characteristic of sulfonate groups (**Figure S3**). [21] Pyridine titration and associated surface IR (DRIFT) vibrational spectroscopy also confirmed that HSPG functionalization enhanced the Brønsted acidity of  $\text{Fe}_3\text{O}_4@\text{SiO}_2@m\text{SiO}_2$  relative to the conventional toluene synthesis (**Figure S4**). We attribute the origin of Lewis acidity to the generation of under-coordinated silicon atoms during the reduction step ( $450 \text{ }^\circ\text{C}$  for 4 h) employed to form the magnetic  $\text{Fe}_3\text{O}_4$  core of our in the synthesis of our  $\text{PrSO}_3\text{H}/\text{Fe}_3\text{O}_4@\text{SiO}_2@m\text{SiO}_2$  catalysts. Such unsaturated  $\text{Si}(\text{O}_3)$  centres exhibit strong Lewis acidity. Post-reduction magnetic nanoparticles were grafted with Brønsted sulfonic acid groups either in toluene (conventional method) or  $\text{NaCl}/\text{H}_2\text{O}$  (HSPG method); the former is expected to preserve Lewis acidic unsaturated Si sites, whereas the latter route is expected to hydroxylate these generating surface silanols (**Scheme 1**). Surface silanols provide additional sites for propyl sulfonic acid functionalization, hence the HSPG method affords strong Brønsted acidity while the conventional method affords mixed Lewis and Brønsted acidity in the final  $\text{PrSO}_3\text{H}/\text{Fe}_3\text{O}_4@\text{SiO}_2@m\text{SiO}_2$  magnetic nanoparticles. Catalytic activity of our magnetic sulfonic acid catalysts was subsequently evaluated for propanoic acid esterification with methanol under mild reaction conditions (**Figure 2**) with associated ester yields and selectivity shown in **Figure S5**, and compared against a non-magnetic, sulfonic acid mesoporous SBA-15 silica ( $\text{PrSO}_3\text{H}/\text{SBA-15}$ ) prepared via the conventional toluene functionalization route. Incorporation of mesoporosity into the magnetic core-silica shell nanoparticles had a striking impact on their esterification performance, imparting a seven-fold rate enhancement for sulfonic acids prepared via grafting in toluene. An additional two-fold increase in the rate of propanoic

acid esterification was achieved for the mesoporous  $\text{Fe}_3\text{O}_4@\text{SiO}_2@m\text{SiO}_2$  catalysts on switching from the toluene to HSPG sulfonic acid protocol.  $\text{Fe}_3\text{O}_4@\text{SiO}_2@m\text{SiO}_2$  (HSPG) delivers a specific (mass normalized) activity which even surpasses that of an entirely mesoporous  $\text{PrSO}_3\text{H/SBA-15}$ , despite the dense iron oxide core of the former magnetic nanoparticles, and 94 % propanoic acid conversion after 6 h reaction. Although all catalysts possess the same propylsulfonic acid active sites, their corresponding Turnover Frequencies (TOFs) shown in **Figure 3** reveal that  $\text{PrSO}_3\text{H/SBA-15}$  and  $\text{Fe}_3\text{O}_4@\text{SiO}_2@m\text{SiO}_2$  (toluene) catalysts exhibit the highest per site reactivity of  $90\text{-}100\text{ h}^{-1}$ , evidencing superior sulfonic acid accessibility; indeed TOFs decrease in the same order as mesopore diameters in **Table 1** ( $5.8 > 2.5 > 1.5 > 1.3\text{ nm}$ ). Remarkably, despite the small diameter of mesopore channels within the outer catalytically active shell of  $\text{Fe}_3\text{O}_4@\text{SiO}_2@m\text{SiO}_2$ (HSPG), its TOF is only half that of the  $\text{PrSO}_3\text{H/SBA-15}$ , suggesting that slower molecular diffusion through the narrower pores of the former is largely compensated for by the significantly shorter channel length ( $60\text{ nm}$  versus  $200\text{ nm}^{-1}\cdot\mu\text{m}$  [20, 23]). There are only two prior reports on magnetic sulfonic acid silica catalysts for carboxylic acid esterification, with performances an order of magnitude lower than our  $\text{Fe}_3\text{O}_4@\text{SiO}_2@m\text{SiO}_2$  catalysts; a TOF of  $4\text{ h}^{-1}$  was reported for oleic acid esterification with methanol at higher temperature over  $\text{Fe/Fe}_3\text{O}_4$  core/shell magnetic nanoparticles possessing a non-porous silica shell co-functionalized by sulfuric and sulfonic acids; [8] and a TOF of  $3.5\text{ h}^{-1}$  and limiting conversion of 40 % for propanoic acid esterification was observed over  $\sim 2\text{ }\mu\text{m}$  magnetic-poly(divinylbenzene-4-vinylpyridine) microbeads treated with sulfuric acid. [24] The combination of mesoporous silica shell and HSPG derivatization route thus represents an attractive route to generate high activity magnetically separable sulfonic acid silica nanoparticles for use in acid catalyzed reactions. Sulfonic acid functionalized silicas prepared by the post-

grafting are known to exhibit relatively poor stability in water generating reactions [25-28], and in common with the literature our  $\text{PrSO}_3\text{H}/\text{Fe}_3\text{O}_4@\text{SiO}_2@m\text{SiO}_2$  catalyst does exhibit a significant drop in propionic acid conversion from 90% to 51% after the second run (**Figure S6**), either due to the instability of propyl sulfonic acid groups (although minimal S leaching was observed by elemental analysis), or strong adsorption of organics within mesopores restricting the accessibility of sulfonic acid. Future work will therefore explore the impact of mesopore diameter (employing poragens and different hydrothermal ageing protocols [29]) on reactivity, and co-condensation routes [21] to improve the thermochemical stability of incorporated sulfonic acid.

#### 4. CONCLUSIONS

In summary, we have demonstrated the first synthesis and catalytic application of magnetically-separable nanoparticles possessing mesoporous sulfonic acid functionalized silica shells. Mesoporosity affords higher sulfonic acid loadings and far superior activity towards propanoic acid esterification than possible employing conventional, non-mesoporous sulfonic acid silica shells, and a catalytic performance comparable to or exceeding that of non-magnetic mesoporous sulfonic acid silicas (the latter of course cannot be readily separated from reaction media). The choice of sulfonate grafting methodology strongly influences both sulfonic acid loadings and corresponding esterification activity, with hydrothermal saline promoted grafting doubling the specific activity with respect to the conventional grafting route.

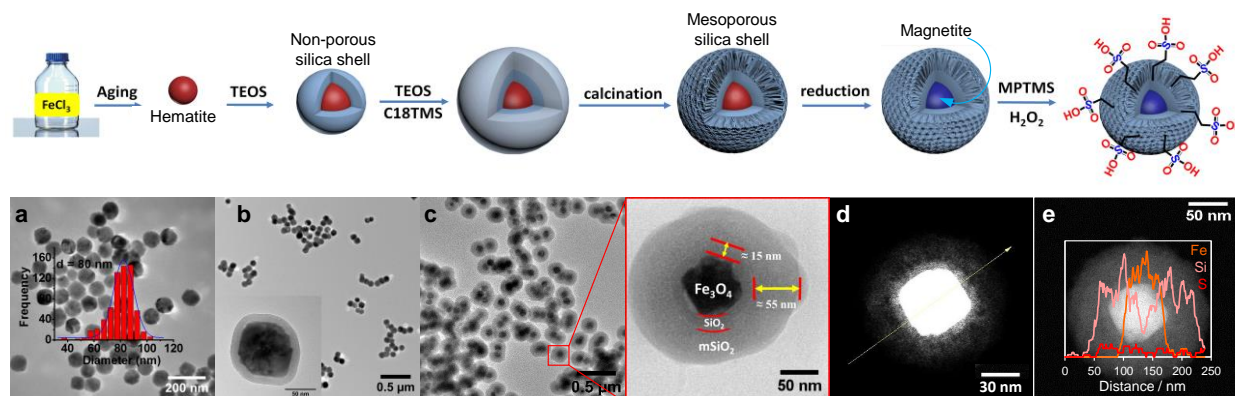
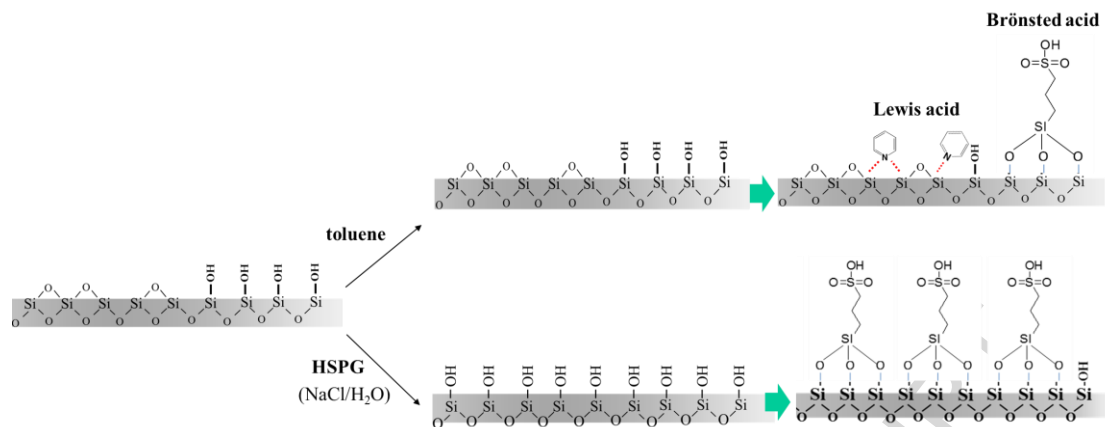


**Figure 1.** Stepwise synthesis of magnetic core-mesoporous shell sulfonic acid silica nanoparticles, and corresponding bright-field TEM images of (a) hematite ( $\text{Fe}_2\text{O}_3$ ), (b)  $\text{Fe}_2\text{O}_3@ \text{SiO}_2$  and (c)  $\text{Fe}_3\text{O}_4@ \text{SiO}_2@m \text{SiO}_2$ , and dark-field TEM images (d-e) of a single  $\text{Fe}_3\text{O}_4@ \text{SiO}_2@m \text{SiO}_2\text{-PrSO}_3\text{H}$  (HSPG) nanoparticle and associated EDX elemental line-scan.



**Scheme 1.** Effect of propyl sulfonic acid grafting route on Lewis and Brønsted acidity of  $\text{PrSO}_3\text{H}/\text{Fe}_3\text{O}_4@\text{SiO}_2@m\text{SiO}_2$  magnetic nanoparticles.

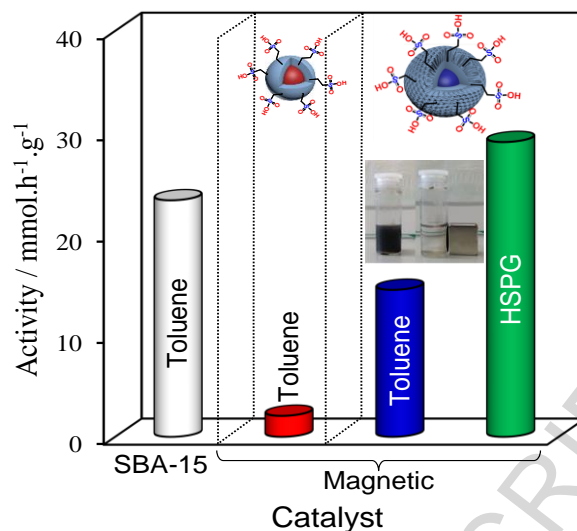


**Figure 2.** Activity of conventional and magnetic non-mesoporous and mesoporous sulfonic acid silicas for propanoic acid esterification with methanol, and (photograph inset) facile magnetic separation of  $\text{Fe}_3\text{O}_4@\text{SiO}_2@m\text{SiO}_2(\text{HSPG})$  post-reaction. Reaction conditions: 60 °C, 10 ml MeOH, 100 mg catalyst, 30:1 molar ratio of MeOH:propanoic acid, 6 h.

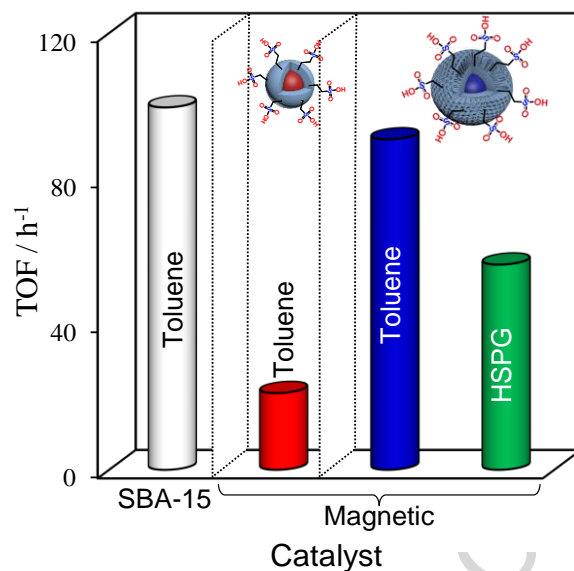


**Figure 3.** TOFs of conventional and magnetic non-mesoporous and mesoporous sulfonic acid silicas for propanoic acid esterification with methanol. Reaction conditions: 60 °C, 10 ml MeOH, 100 mg catalyst, 30:1 molar ratio of MeOH:propanoic acid, 6 h.

**Table 1.** Surface and bulk properties of magnetic solid acid catalysts

Entry	Samples	$S_{\text{BET}}^c / \text{m}^2 \cdot \text{g}^{-1}$	Pore volume/ $\text{cm}^3 \cdot \text{g}^{-1}$	BJH pore diameter <sup>d</sup> / nm	S surface content <sup>e</sup> / Atom %	S bulk content <sup>f</sup> / wt. %	Acid site loading <sup>g</sup> / $\text{mmol} \cdot \text{g}^{-1}$
1	$\text{Fe}_3\text{O}_4@\text{SiO}_2@\text{mSiO}_2$	419.8	0.520	3.09	-	-	-
2	$\text{Fe}_2\text{O}_3@\text{SiO}_2$	45.0	0.130	3.86	-	-	-
3	$\text{Fe}_3\text{O}_4@\text{SiO}_2@\text{mSiO}_2$ (toluene) <sup>a</sup>	374.4	0.405	2.49	0.17	0.25	0.16
4	$\text{Fe}_2\text{O}_3@\text{SiO}_2$ (toluene) <sup>a</sup>	75.8	0.088	1.30	0.12	0.05	0.09
5	$\text{Fe}_3\text{O}_4@\text{SiO}_2@\text{mSiO}_2$ (HSPG) <sup>b</sup>	323.9	0.305	1.54	0.80	1.35	0.51
6	$\text{Fe}_2\text{O}_3@\text{SiO}_2$ (HSPG) <sup>b</sup>	53.7	0.146	3.82	0.33	0.55	0.32
7	SBA-15-PrSO <sub>3</sub> H	742	1.004	5.82	0.38	0.95	0.23

<sup>a</sup>Sulfonic nanoparticles prepared by conventional method (toluene). <sup>b</sup>Sulfonic nanoparticles prepared by NaCl/H<sub>2</sub>O method (HSPG). <sup>c</sup>N<sub>2</sub> porosimetry. <sup>d</sup>BJH analysis of desorption branch of isotherm. <sup>e</sup>XPS. <sup>f</sup>CHNS elemental analysis. <sup>g</sup>Propylamine TGA-MS.

**Supporting Information.**

Material synthesis, experimental details, XRD, FTIR, porosimetry, TGA-MS, XPS and additional reaction data is available.

Underpinning data is also available at the following link: <http://dx.doi.org/10.17036/a497b0ab-45ba-409d-8b41-9ff1ad6656e0>

**AUTHOR INFORMATION****ACKNOWLEDGMENTS**

We thank the EPSRC for financial support under EP/K014676/1 and the Royal Society for the award of an Industry Fellowship to KW.

## REFERENCES

- [1] J.H. Clark, *Solid Acids for Green Chemistry*, *Acc. Chem. Res.*, 35 (2002) 7.
- [2] M.B. Gawande, Y. Monga, R. Zboril, R.K. Sharma, Silica-decorated magnetic nanocomposites for catalytic applications, *Coord Chem Rev*, 288 (2015) 118-143.
- [3] V. Polshettiwar, R. Luque, A. Fihri, H. Zhu, M. Bouhrara, J.-M. Basset, Magnetically Recoverable Nanocatalysts, *Chemical Reviews*, 111 (2011) 3036-3075.
- [4] D.-m. Lai, L. Deng, Q.-x. Guo, Y. Fu, Hydrolysis of biomass by magnetic solid acid, *Energy Environ. Sci.*, 4 (2011) 3552-3557.
- [5] X. Zhang, M. Wang, Y. Wang, C. Zhang, Z. Zhang, F. Wang, J. Xu, Nanocoating of magnetic cores with sulfonic acid functionalized shells for the catalytic dehydration of fructose to 5-hydroxymethylfurfural, *Chin J Catal*, 35 (2014) 703-708.
- [6] S. Wang, Z. Zhang, B. Liu, J. Li, Silica coated magnetic Fe<sub>3</sub>O<sub>4</sub> nanoparticles supported phosphotungstic acid: a novel environmentally friendly catalyst for the synthesis of 5-ethoxymethylfurfural from 5-hydroxymethylfurfural and fructose, *Catal. Sci. Technol.*, 3 (2013) 2104.
- [7] R. Fang, R. Luque, Y. Li, Selective aerobic oxidation of biomass-derived HMF to 2,5-diformylfuran using a MOF-derived magnetic hollow Fe-Co nanocatalyst, *Green Chem.*, 18 (2016) 3152-3157.
- [8] H. Wang, J. Covarrubias, H. Prock, X. Wu, D. Wang, S.H. Bossmann, Acid-Functionalized Magnetic Nanoparticle as Heterogeneous Catalysts for Biodiesel Synthesis, *J. Phys. Chem. C*, 119 (2015) 26020-26028.
- [9] Zillillah, G. Tan, Z. Li, Highly active, stable, and recyclable magnetic nano-size solid acid catalysts: efficient esterification of free fatty acid in grease to produce biodiesel, *Green Chemistry*, 14 (2012) 3077-3086.
- [10] Q. Zhang, J. Chang, T. Wang, Y. Xu, Review of biomass pyrolysis oil properties and upgrading research, *Energy Convers. Manage.*, 48 (2007) 87-92.
- [11] L. Ciddor, J.A. Bennett, J.A. Hunns, K. Wilson, A.F. Lee, Catalytic upgrading of bio-oils by esterification, *J. Chem. Technol. Biotechnol.*, 90 (2015) 780-795.
- [12] S. Miao, B.H. Shanks, Esterification of biomass pyrolysis model acids over sulfonic acid-functionalized mesoporous silicas, *Applied Catalysis A: General*, 359 (2009) 113-120.
- [13] G. Cheng, J.-L. Zhang, Y.-L. Liu, D.-H. Sun, J.-Z. Ni, Synthesis of novel Fe<sub>3</sub>O<sub>4</sub>@SiO<sub>2</sub>@CeO<sub>2</sub> microspheres with mesoporous shell for phosphopeptide capturing and labeling, *Chem. Commun.*, 47 (2011) 5732-5734.
- [14] S. Wu, H. Wang, S. Tao, C. Wang, L. Zhang, Z. Liu, C. Meng, Magnetic loading of tyrosinase-Fe<sub>3</sub>O<sub>4</sub>/mesoporous silica core/shell microspheres for high sensitive electrochemical biosensing, *Anal. Chim. Acta*, 686 (2011) 81-86.
- [15] R.-Y. Hong, J.-H. Li, S.-Z. Zhang, H.-Z. Li, Y. Zheng, J.-m. Ding, D.-G. Wei, Preparation and characterization of silica-coated Fe<sub>3</sub>O<sub>4</sub> nanoparticles used as precursor of ferrofluids, *Appl. Surf. Sci.*, 255 (2009) 3485-3492.
- [16] A. Takagaki, M. Nishimura, S. Nishimura, K. Ebitani, Hydrolysis of sugars using magnetic silica nanoparticles with sulfonic acid groups, *Chem. Lett.*, 40 (2011) 1195-1197.
- [17] P.S. Mueller, C.P. Parker, S.C. Larsen, One-pot synthesis of iron oxide mesoporous silica core/shell nanocomposites, *Microporous and Mesoporous Materials*, 204 (2015) 173-179.
- [18] J. Kim, H.S. Kim, N. Lee, T. Kim, H. Kim, T. Yu, I.C. Song, W.K. Moon, T. Hyeon, Multifunctional uniform nanoparticles composed of a magnetite nanocrystal core and a

mesoporous silica shell for magnetic resonance and fluorescence imaging and for drug delivery, *Angewandte Chemie*, 47 (2008) 8438-8441.

[19] W.R. Zhao, J.L. Gu, L.X. Zhang, H.R. Chen, J.L. Shi, Fabrication of uniform magnetic nanocomposite spheres with a magnetic core/mesoporous silica shell structure, *J. Am. Chem. Soc.*, 127 (2005) 8916-8917.

[20] D. Zhao, J. Feng, Q. Huo, N. Melosh, G.H. Fredrickson, B.F. Chmelka, G.D. Stucky, Triblock copolymer syntheses of mesoporous silica with periodic 50 to 300 angstrom pores, *science*, 279 (1998) 548-552.

[21] C. Pirez, A.F. Lee, J.C. Manayil, C.M.A. Parlett, K. Wilson, Hydrothermal saline promoted grafting: a route to sulfonic acid SBA-15 silica with ultra-high acid site loading for biodiesel synthesis, *Green Chem.*, 16 (2014) 4506-4509.

[22] C. Pirez, M.T. Reche, A.F. Lee, J.C. Manayil, V.C. dos-Santos, K. Wilson, Hydrothermal Saline Promoted Grafting of Periodic Mesoporous Organic Sulfonic Acid Silicas for Sustainable FAME Production, *Catalysis Letters*, 145 (2015) 1483-1490.

[23] J. Dhainaut, J.-P. Dacquin, A.F. Lee, K. Wilson, Hierarchical macroporous–mesoporous SBA-15 sulfonic acid catalysts for biodiesel synthesis, *Green Chemistry*, 12 (2010) 296-303.

[24] A. Kara, B. Erdem, Synthesis, characterization and catalytic properties of sulfonic acid functionalized magnetic-poly(divinylbenzene-4-vinylpyridine) for esterification of propionic acid with methanol, *Journal of Molecular Catalysis A: Chemical*, 349 (2011) 42-47.

[25] A.J. Crisci, M.H. Tucker, M.-Y. Lee, S.G. Jang, J.A. Dumesic, S.L. Scott, Acid-Functionalized SBA-15-Type Silica Catalysts for Carbohydrate Dehydration, *ACS Catalysis*, 1 (2011) 719-728.

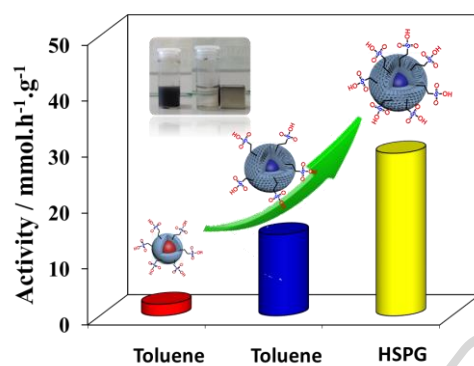
[26] A. Karam, J.C. Alonso, T.I. Gerganova, P. Ferreira, N. Bion, J. Barrault, F. Jerome, Sulfonic acid functionalized crystal-like mesoporous benzene-silica as a remarkable water-tolerant catalyst, *Chemical Communications*, (2009) 7000-7002.

[27] C. Bispo, K. De Oliveira Vigier, M. Sardo, N. Bion, L. Mafra, P. Ferreira, F. Jerome, Catalytic dehydration of fructose to HMF over sulfonic acid functionalized periodic mesoporous organosilicas: role of the acid density, *Catalysis Science & Technology*, 4 (2014) 2235-2240.

[28] A.J. Crisci, M.H. Tucker, J.A. Dumesic, S.L. Scott, Bifunctional Solid Catalysts for the Selective Conversion of Fructose to 5-Hydroxymethylfurfural, *Topics in Catalysis*, 53 (2010) 1185-1192.

[29] J.P. Dacquin, A.F. Lee, C. Pirez, K. Wilson, Pore-expanded SBA-15 sulfonic acid silicas for biodiesel synthesis, *Chemical Communications*, 48 (2012) 212-214.

## Graphical abstract



### Highlights

- Magnetically-separable mesoporous sulfonic acid derivatised nanoparticles.
- Enhanced sulfonic acid loadings via hydrothermal saline promoted grafting method.
- Superior esterification activity compared to non-porous magnetic nanoparticles.

ACCEPTED MANUSCRIPT